HOW LLMS LEARN TO REASON: A COMPLEX NETWORK PERSPECTIVE

Sihan Hu[1,2]*, **Xiansheng Cai**[3*], **Yuan Huang**[5]†, **Zhiyuan Yao**[7]‡, **Linfeng Zhang**[5,6]§, **Pan Zhang**[3,4]¶
Youjin Deng[1,2]‖, **Kun Chen**[3**]
[1]Department of Modern Physics, University of Science and Technology of China
[2]Hefei National Laboratory
[3]Institute of Theoretical Physics, Chinese Academy of Sciences
[4]School of Fundamental Physics and Mathematical Sciences, Hangzhou Institute for Advanced Study
[5]DP Technology
[6]AI for Science Institute, Beijing
[7]Lanzhou Center for Theoretical Physics, Key Laboratory of Theoretical Physics of Gansu Province,
Key Laboratory of Quantum Theory and Applications of MoE,
Gansu Provincial Research Center for Basic Disciplines of Quantum Physics, Lanzhou University
huangyuan@dp.tech, yaozy@lzu.edu.cn, zhanglf@dp.tech, panzhang@itp.ac.cn,
yjdeng@ustc.edu.cn, chenkun@itp.ac.cn

ABSTRACT

Training large language models with Reinforcement Learning from Verifiable Rewards (RLVR) exhibits a set of distinctive and puzzling behaviors that remain poorly understood, including a two-stage learning curve, V-shaped response-length trajectories, and a pronounced vulnerability to catastrophic forgetting. In this work, we propose that these seemingly disparate phenomena can be explained using a single unifying theory: the model's reasoning process maps to the self-organization of a semantic complex network whose topology remains persistently sparse, with the average degree pinned close to two. This topology imposes a fundamental mechanism for forgetting and learning: it first drives the system into a maximally frustrated state where "skill islands" form, slow-learning happens, and forgetting is induced; then it enters a sharp growth phase where the new skills are "bolted on", driven by phase-transition-like learning at the web's frontier. Equipped with the theory, we propose *Annealed-RLVR*, a principled algorithm that introduces an SFT-based "heating" step at the point of maximal frustration to resolve the competitive bottleneck and enhance the reasoning capability of the model. Experiments on a 1.5B-parameter model demonstrate that the approach outperforms standard RLVR on both in-distribution and out-of-distribution benchmarks. By recasting RLVR from black-box optimization into a predictable process of structural self-organization, our work provides a new physical intuition for engineering the emergent reasoning capabilities of future AI systems.

*These authors contributed equally to this paper.
†Corresponding Author
‡Corresponding Author
§Corresponding Author
¶Corresponding Author
‖Corresponding Author
**Corresponding Author

1 INTRODUCTION

Large language models (LLMs) trained with Reinforcement Learning from Verifiable Rewards (RLVR) (Liu et al., 2025; Guo et al., 2025; Team et al., 2025; Yang et al., 2025) are increasingly capable of multi-step, "System-2" reasoning. Yet, this training paradigm consistently exhibits a set of puzzling macroscopic behaviors across diverse architectures and benchmarks. These include (i) rapid initial gains that give way to a prolonged plateau; (ii) a V-shaped trajectory in the length of correct solutions, which first shortens before steadily lengthening (Luo et al., 2025; He et al., 2025; Fatemi et al., 2025); and (iii) a pronounced vulnerability to catastrophic forgetting when interleaved with supervised fine-tuning (SFT) (Li & Hoiem, 2017; Fernando et al., 2025; Ding & Wang, 2025). Although these phenomena are widely observed, the reasons for their co-occurrence remain elusive. A clear understanding of the underlying mechanism would be essential for developing more efficient approaches to training reasoning-capable models.

A promising theoretical framework analyzes these phenomena by modeling the LLM's reasoning process on an implicit reasoning graph — a network of semantic states and logical transitions(Wang et al., 2024; Dutta et al., 2024; Xiang et al., 2025; Cabannes et al., 2024; Minegishi et al., 2025). However, this perspective faces a critical roadblock: a direct, microscopic analysis is currently intractable. Constructing this entire graph from a model's high-dimensional latent space remains a formidable open problem, preventing a direct investigation into the structural origins of the observed dynamics.

Here, we argue that the very universality of the RLVR phenomena provides a path forward. In complex systems, behaviors that are independent of microscopic details are often emergent properties, governed by the system's large-scale organization (Anderson, 1972; Watts & Strogatz, 1998; Barabási & Albert, 1999). This insight motivates an approach rooted in the core logic of the Renormalization Group (RG)(Wilson & Kogut, 1974): instead of getting bogged down by intractable local details, one can leap directly to hypothesizing a core principle about the system's large-scale structure to explain its macroscopic behavior. Applying this strategy, we shift our focus from the full reasoning graph to its coarse-grained backbone, which emerges by abstracting away fine-grained skills encoded in local network patterns like motifs or community structures. This leads us to our central hypothesis regarding the emergent structure that forms under RLVR training for general-purpose System-2 reasoning:

Hypothesis 1. *The **concept web**, defined as the coarse-grained reasoning graph, is a sparse network whose effective average degree is pinned to* $\langle k \rangle \approx 2$.

The implications of this hypothesis are non-trivial: an average degree of 2 implies a predominantly tree-like structure, which is efficient for generalization but inherently fragile. This topology can still support rare, large-scale cycles critical for complex operations like self-correction (as detailed in Appendix C), without significantly altering the global average degree.

To validate this hypothesis, we combine two approaches: a theoretical study using the Concept Network Model (CoNet) (Cai et al., 2025), a minimal "computational microscope" that reproduces the LLM's core training dynamics, and numerical experiments on a 1.5B-parameter LLM(Luo et al., 2025). This dual approach reveals a clear structural narrative for the observed puzzles. The learning plateau is shown to be the arduous consolidation of disconnected "skill islands", a transition that directly explains the V-shaped length trajectory. Furthermore, the resulting sparse, tree-like concept web accounts for the model's fragility and its vulnerability to catastrophic forgetting with SFT.

This sparse topology imposes a microscopic dynamic of learning and forgetting that is a hallmark of the RLVR-driven self-organization process. We find the degree-2 constraint first forces the system into a maximally frustrated state at the onset of the slow-learning plateau, a phase dominated by **frustration-induced forgetting** as skills are competitively suppressed. Subsequently, the very same structure enables the growth

mechanism that governs the entire slow-learning phase: a steady, sequential process where new skills are individually "bolted on" at the web's expanding frontier via a **phase-transition-like learning** dynamic.

Equipped with the sparse-web theory, we propose Annealed-RLVR, a principled algorithm that introduces an SFT-based "heating" step at the point of maximal frustration to resolve the competitive bottleneck and enhance exploration and reasoning efficacy of the subsequent RLVR phase. Experiments on both CoNet and the 1.5B-parameter LLM confirm the efficacy of this strategy: Annealed-RLVR surpasses standard RLVR on both in-distribution and out-of-distribution benchmarks, transforming our physical intuition into a practical tool for engineering emergent reasoning.

2 The V-Shaped Signature as Evidence for a Sparse Concept Web

The V-shaped evolution of response length is a well-demonstrated, quantifiable hallmark of deep structural reorganization during RLVR training(He et al., 2025; Luo et al., 2025). To anchor our investigation, we first reproduce this signature by applying RLVR to the DeepSeek-R1-Distill-Qwen-1.5B model following the DeepScaleR protocol (Luo et al., 2025). As shown in Fig. 1, our experiment recovers the characteristic V-shaped curve (Fig. 1). We contend that this is not a mere by-product but the primary empirical evidence for our central claim: the emergence of a sparse, unified concept web.

To dissect the mechanism underlying this signature—a task intractable within the LLM itself—we deploy an extended, multi-task variant of the CoNet as a "computational microscope" (See Appendix D for details). This minimal model reduces the learning process to a tractable graph-traversal problem and, remarkably, reproduces the V-shaped curve observed in our LLM experiment (Fig. 1), validating it as a faithful proxy for uncovering the underlying mechanism.

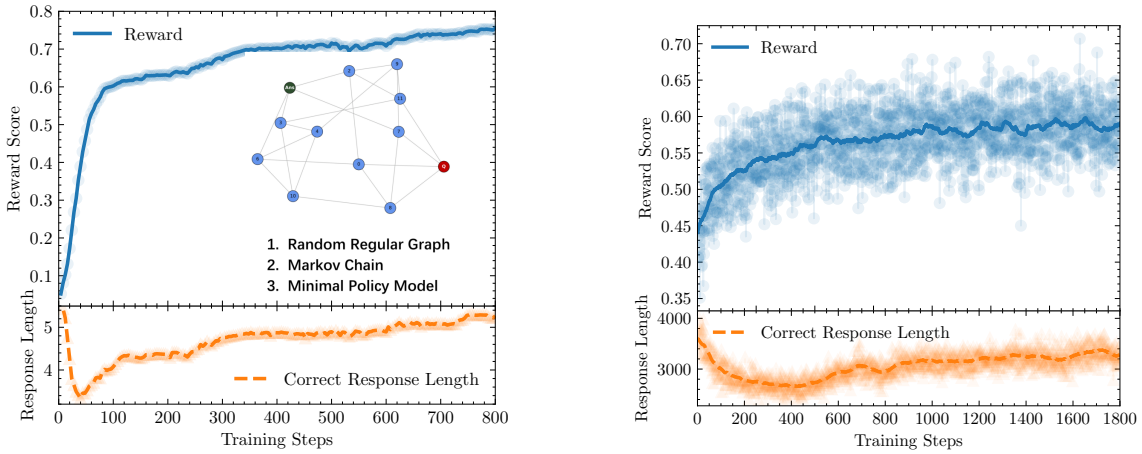

(a) CoNet (b) LLM

Figure 1: **CoNet Faithfully Reproduces Core LLM Training Dynamics.** The minimal CoNet model (a) remarkably reproduces the two core empirical signatures of RLVR training observed in the DeepScaleR-1.5B LLM (b). These signatures are: (i) a two-stage reward dynamic consisting of a fast-learning phase followed by a slow-learning plateau (top panels), and (ii) a non-monotonic, V-shaped evolution of the correct response length (bottom panels). This striking correspondence validates CoNet as a tractable minimal model for our theoretical analysis. The inset in (a) schematically depicts the CoNet abstraction. Lines in (b) are smoothed with a 60-step moving average.

Armed with this confirmation, we now expose the topological origin of the V-shape. The V-shaped curve arises from a distinct two-stage process. During the initial fast-learning phase where response length decreases, the model undergoes local optimization: it rapidly discovers short, efficient solutions to individual problems, giving rise to a proliferation of disconnected "skill islands" (as shown in Fig. 2(a)). This burst is quantified by the number of distinct solution clusters, which peaks right before the onset of slow learning (Fig. 2(b)). Stage one thus constitutes a parallel search for local efficiency that naturally drives down the average response length.

The subsequent slow-learning phase, where response length steadily increases, marks a fundamental shift to global integration. The primary task is no longer discovering new islands but weaving them into a single, expansive concept web (see Fig. 2(c)). As the largest connected component relentlessly grows, a critical structural property emerges: the web remains persistently sparse, with its average degree stabilizing near two (as shown in Fig. 3(c)). This provides direct, quantitative validation for our central Hypothesis (Hypothesis 1).

This emergent sparsity is the topological key to the V-shape's rising slope. A network with such a low average degree is dominated by chain and tree-like structures, inherently lacking the shortcuts and redundant pathways found in denser graphs. Consequently, connecting two previously distant concepts requires traversing long, intermediate paths. The histograms in Fig. 3(a) provide dispositive proof of this effect: As the sparse web expands, the distribution of solution lengths undergoes a decisive and sustained rightward shift, confirming that navigation on this sparse backbone necessitates longer reasoning chains. Thus, the V-shaped curve furnishes a robust macroscopic signature of an underlying topological transition: from parallel, local optimization on disconnected components to serial, global navigation across an expanding, sparse backbone.

Yet can this simple, largely tree-like model capture the full complexity of LLM reasoning? After all, an LLM's autoregressive memory enables sophisticated behaviors such as self-correction or reflection (e.g., "Wait, let me rethink that...")—that would manifest as cycles in the reasoning graph. We argue they are fully compatible(Minegishi et al., 2025). These reasoning cycles are not the dense, ubiquitous shortcuts

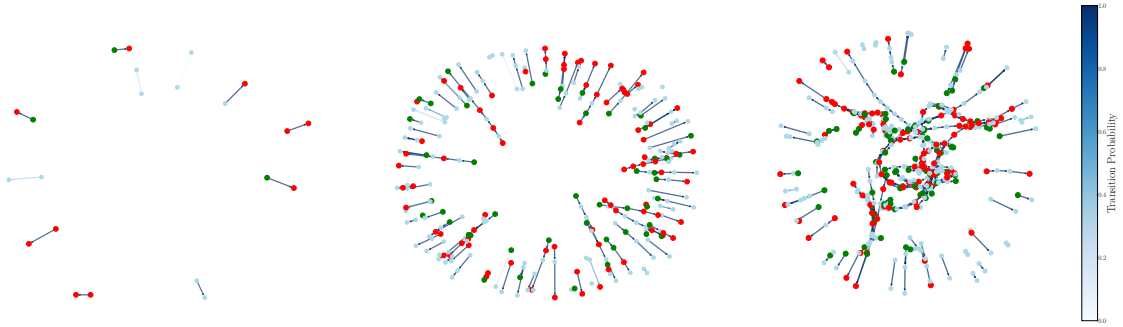

(a) Step 20 (b) Step 50 (c) Step 800

Figure 2: **Visualizing the Structural Evolution from Skill Islands to the Concept Web.** These network snapshots provide a direct, qualitative narrative of the concept web's formation, corresponding to the different phases of training. **(a)** In the early fast-learning phase (Step 20), the model discovers a few short, disjointed reasoning paths, representing the first nascent "skill islands". **(b)** At the onset of slow learning (Step 50), the system has proliferated into a maximal collection of disconnected islands. **(c)** Deep in the slow-learning phase (Step 800), these previously separate islands have coalesced into a single, giant connected component, forming the unified and expansive concept web.

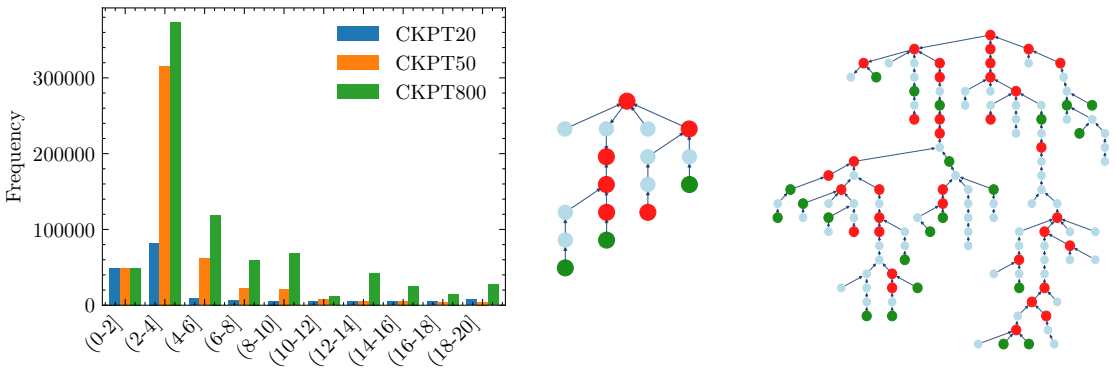

(a) Correct Response Histogram (b) Step 50 (c) Step 800

Figure 3: **A Sparse Web Structure Necessitates Longer Reasoning Chains.** This figure links the emergent sparse topology of the concept web to the observed increase in response length. (b, c) The largest connected component (edges with probability > 0.95) remains sparse (average degree ≈ 2) even as it grows from step 50 to 800. (a) Consequently, the distribution of solution path lengths shifts decisively to the right during this period, confirming that navigating the sparse backbone requires longer reasoning chains.

of a highly connected graph. Instead, they are likely the cognitive manifestation of sparse, local loops—occasional, high-cost revisions on a much larger, fundamentally chain-like scaffold. The existence of a limited number of such cycles does not significantly alter the global average degree of the web, which remains close to two. With the sparse web model established, this link between a macroscopic dynamic and a microscopic topology forms the foundation for the analysis that follows.

3 The Double-Edged Sword of Sparsity: from Catastrophic Forgetting to Simulated Annealing scheme

From the graph theoretic point of view, the sparsity in the conceptual network implies low redundancy, fragility, and critical vulnerability. It also reflects a structural hypothesis for a well-known operational challenge: why models that have formed a concept web via RLVR are so susceptible to catastrophic forgetting when subsequently fine-tuned with (Li et al., 2024). Our theory posits that this is not a widespread erasure of knowledge, but a specific topological failure: the surgical severing of critical, bridge-like connections.

To test this mechanistic hypothesis, we subjected models in the deep slow-learning phase to a lightweight in-distribution SFT (see Appendix H and I). As expected, the intervention triggered a precipitous collapse in overall performance in both CoNet and the 1.5B LLM (Fig. 4(a), (b)). Having reproduced this known macroscopic phenomenon, we leveraged CoNet's transparency to inspect the microscopic aftermath.

The result is a direct validation of our structural explanation. The microscopic view reveals that the SFT catastrophic forgetting was not a global degradation of the web. Instead, SFT's aggressive optimization of a few paths overwrote the policy at critical branching nodes, surgically severing the single connection points for vast downstream subgraphs. Fig. 4(c), (d) provides a stark visualization of this: a unified web is instantly fragmented, offering a clear, structural cause for the catastrophic performance drop.

However, this is where the sword's second edge is revealed. The damage, while profound in its effect, is topologically localized. SFT does not erase the knowledge encoded in the now-disconnected subgraphs; it merely renders them unreachable. This localization explains the remarkable speed of recovery, which can

be observed in Fig. 4(a), (b). When RLVR training resumes, it triggers a quick rebound because the task is simply to "re-solder" a few broken connections to restore access to the latent scaffold as shown in Fig. 4(e).

This two-step process of localized disruption followed by rapid repair is strongly analogous to simulated annealing Kirkpatrick et al. (1983). The brief SFT phase acts as a high-temperature "heating" shock, breaking connections and allowing the system to escape a potentially suboptimal state. The subsequent RLVR phase then acts as a controlled "cooling", guiding the system as it re-forms connections, ideally settling into a more robust configuration (Lai et al., 2025). This insight—that a known vulnerability can be repurposed as a deliberate annealing step—forms the foundation for the Annealed-RLVR algorithm, which we introduce in Sec.5.

4 Microscopic Mechanisms of RLVR: Forgetting by Frustration, Learning by Phase Transition

Our sparse web theory reveals that the smooth, aggregate reward curve of RLVR training masks a dramatic microscopic behavior. Individual problem trajectories in Fig. 5 reveal a fundamental tension born from the

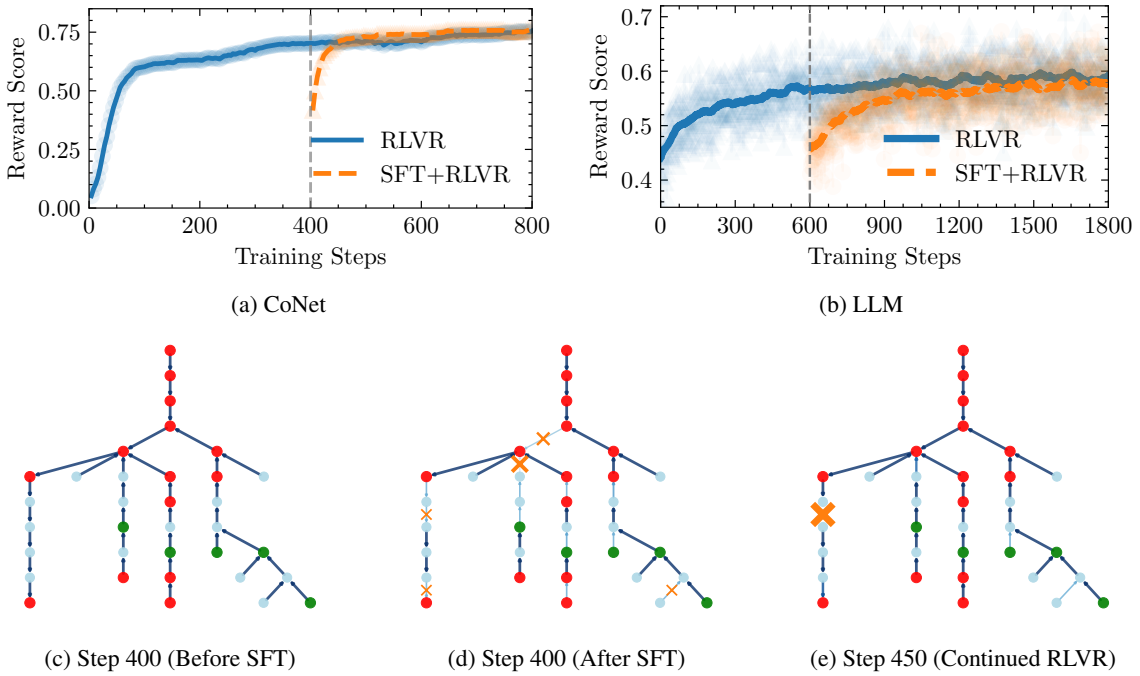

(a) CoNet (b) LLM

(c) Step 400 (Before SFT) (d) Step 400 (After SFT) (e) Step 450 (Continued RLVR)

Figure 4: **The Fragility of a Sparse Web: Catastrophic Forgetting and Fast Recovery.** This figure demonstrates a key prediction of our sparse web hypothesis: that the concept web is fragile, relying on critical bridge-like connections. (c-e) The microscopic view in CoNet shows how a lightweight supervised fine-tuning (SFT) on a converged web (c) severs these critical bridges, causing the structure to fragment (d). Subsequent RLVR rapidly repairs these links (e). (a, b) This microscopic severing manifests as macroscopic catastrophic forgetting in both CoNet and the 1.5B LLM, where performance collapses upon initiating SFT. The subsequent fast recovery once RLVR resumes highlights the localized nature of the damage, underscoring the web's structural fragility.

network's sparse topology: a subtractive process of frustration-induced forgetting, peaking at the onset of slow learning, and an opposing, additive process of phase-transition-like learning that drives knowledge integration throughout the slow-learning stage.

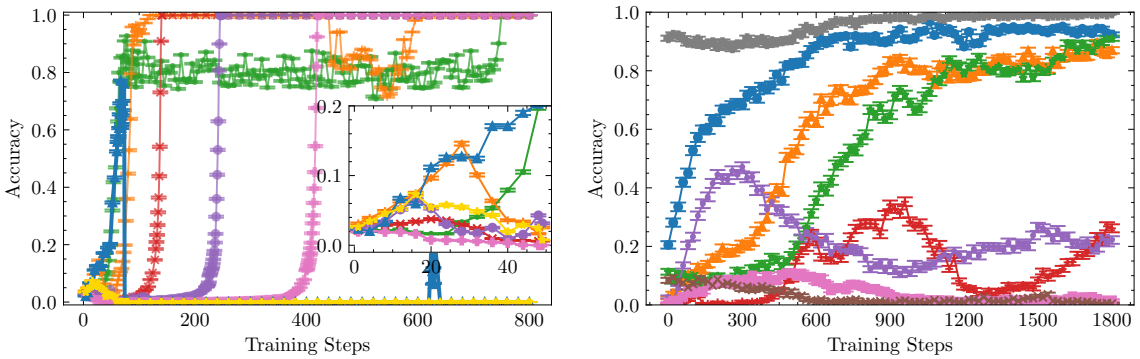

(a) CoNet (b) LLM

Figure 5: **Microscopic Mechanisms of RLVR: Forgetting by Frustration, Learning by Phase Transition** The learning trajectories for individual problems in CoNet (a) and the 1.5B LLM (b) reveal a fundamental duality. (i) Frustration-Induced Forgetting: At the transition to slow learning (see inset in (a)), the intense competition for connections on a sparse web manifests as volatile, non-monotonic accuracy curves, where some skills are competitively suppressed. (ii) Phase-Transition-Like Learning: Subsequently, the web's sparse frontier enables new skills to be acquired in punctuated, accelerated jumps (orange and green). The smoother gradients in the LLM (vs. the clean steps in CoNet) can be attributed to a classic finite-size effect, as explained in the main text.

4.1 Frustration-Induced Forgetting: The Price of Integration

The first dynamic is driven by frustration-induced forgetting: a competitive process where the advancement of some skills forces the deterministic regression of others as the model integrates its "skill islands". This process manifests as volatile, non-monotonic learning curves in the learning dynamics (Fig. 5) and represents an internal "push-and-pull" fundamentally different from the external shock of SFT-induced catastrophic forgetting (Shenfeld et al., 2025; Jin et al., 2025).

This process peaks in the maximally frustrated state at the onset of the slow-learning stage, a critical juncture where skill islands compete for limited connections under the $\langle k \rangle \approx 2$ constraint. Paradoxically, this state maximizes exploration: the model's ability to find diverse, correct out-of-distribution solutions peaks, far exceeding the base model or the same model after prolonged training (Fig. 6(b), blue). This subsequent degradation in performance is consistent with the phenomenon of policy collapse, which has been recently reported in several studies to occur after extended RLVR, leading to a loss of exploratory power (Chen et al., 2025; Yue et al., 2025; Cui et al., 2025).

4.2 Phase-Transition-Like Learning: The Engine of Growth

The opposing dynamic, phase-transition-like learning, is an important engine of new knowledge acquisition (Power et al., 2022; Lin et al., 2025). The evidence for this is clearly shown in CoNet's sharp, step-like accuracy jumps (Fig. 5(a)), and the steep accelerated learning gradients observed in the 1.5B LLM (Fig. 5(b), more details in Appendix G). This phenomenon is a multi-task extension of the "Learning at Criticality"

(LaC) mechanism, first identified in a single-task context (Cai et al., 2025). The LaC framework models this process as a continuous phase transition(Stanley & Ahlers, 1972; Wilson, 1983) where the policy collapses from exploring diverse reasoning paths to exploiting a single optimal one. Crucially, analysis revealed that near this critical point, the system's exploratory power is maximized, and the reasoning path lengths become scale-invariant—a hallmark of continuous phase transitions. This context explains the smoother gradient in the LLM. Compared to the step-like jumps in CoNet, the LLM's learning curve is a classic manifestation of a finite-size effect(Fisher & Barber, 1972): it has a more constrained set of distinct reasoning paths for any given task, which rounds out the idealized sharp transition into a steep but continuous curve.

The puzzle is why this delicate phenomenon survives in a chaotic multi-task setting. Our sparse-web model explains this through topological isolation: a node on the expanding frontier of a $\langle k \rangle \approx 2$ network is statistically isolated, decoupling it from system-wide competition. Shielded from interference, a new skill can be efficiently "bolted on" via a clean phase transition. This perspective also provides a microscopic explanation for aggregate policy collapse in the standard RLVR (Chen et al., 2025; Yue et al., 2025; Cui et al., 2025). We hypothesize this is not a monolithic failure but the statistical sum of asynchronous, microscopic collapses at the frontier, a hypothesis supported by the LaC finding that training just beyond criticality risks overfitting-induced collapse.

5 Annealed-RLVR: An Algorithm Born from the Sparse Web Theory

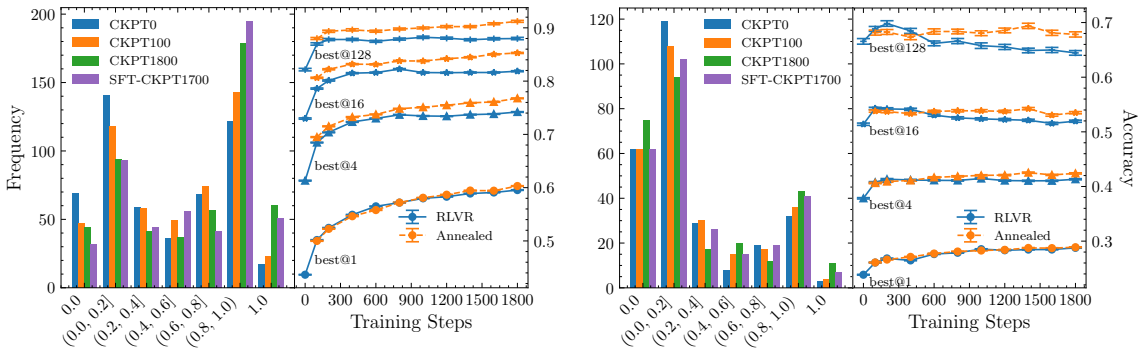

(a) Randomly Selected 512 Training Problems

(b) Minerva

Figure 6: **Annealed-RLVR Outperforms Standard RLVR.** This figure compares our Annealed-RLVR ("Annealed") with a standard RLVR baseline ("RLVR") on (a) in-distribution problems and (b) the out-of-distribution Minerva dataset. (Right panels) The best@k accuracy curves show that Annealed-RLVR achieves superior performance in both settings, confirming improved generalization. (Left panels) The histograms reveal the underlying mechanism: the annealing intervention systematically reduces the population of unsolved problems (low-accuracy bins) and improves the mastered ones (high-accuracy bins).

Our sparse-web theory reveals a core narrative of RLVR training: the system drives itself into a maximally frustrated state that is both a perilous bottleneck and a moment of peak exploratory potential (Fig. 6(b), blue curve). This insight motivates Annealed-RLVR, a theory-driven intervention that leverages the high-entropy frustrated state to guide the model toward a more globally optimal configuration (Cheng et al., 2025; Chen et al., 2025).

The algorithm operationalizes this concept with a precisely timed intervention, triggered by macroscopic signatures of the maximally frustrated state. At this juncture, a brief SFT "heating" phase begins. The timing is critical: because the "skill islands" have not yet solidified into a single web, the system is uniquely robust

to a targeted shock that would otherwise cause catastrophic forgetting—a theoretical claim confirmed by our experiments (Fig. 4). The SFT thus functions not as a disruptive overwrite but as a corrective jolt to break the policy's premature commitment to suboptimal routes. We implement this by surgically applying SFT only to problems with low accuracy (e.g., < 0.1) for which correct solutions exist. Immediately following this targeted heating, the "cooling" stage resumes standard RLVR, allowing the now more pliable policy to re-settle into a more robust and integrated final state.

The results validate this theory-driven approach (Fig. 6). Best@k accuracy curves demonstrate that Annealed-RLVR outperforms standard RLVR on both in-distribution problems and, crucially, the out-of-distribution Minerva dataset, confirming the intervention fosters true generalization. The histograms reveal the underlying mechanism: the SFT "heating" provides a crucial performance boost to the most difficult problems, lifting their success rates from near-zero and making them "visible" to subsequent RLVR exploration. The RLVR "cooling" phase then efficiently guides these newly accessible problems toward mastery. This results in a systematic reduction of unsolved problems and a corresponding population shift towards solved ones, confirming that our intervention guides the model past the inherent bottlenecks of standard RLVR to achieve superior reasoning. More details are given in Appendix H and I.

6 Conclusion and Outlook

We have introduced a sparse-concept-net theory to explain the puzzling behaviors of the RLVR training, including the two-stage learning curve, V-shaped response curves, and vulnerability to catastrophic forgetting. Our theory proposes that these diverse phenomena are consequences of one underlying process: the formation of a sparse concept web, with the averaged degree pinned close to two. This physical model directly explains the V-shaped curve as a shift from local optimization to global integration and recasts catastrophic forgetting as the severing of the web's critical, bridge-like connections.

A natural consequence of this sparse structure is a fundamental RLVR mechanism for forgetting and learning within the microscopic training process. We find that the degree-2 constraint first forces the system into a maximally frustrated state at the onset of slow learning, a phase dominated by frustration-induced forgetting as skills are competitively suppressed. Subsequently, the same sparse structure enables a cleaner growth mechanism: phase-transition-like learning, where new knowledge is efficiently "bolted on" at the web's expanding frontier.

This framework is not just descriptive; it is prescriptive. It identifies the maximally frustrated state—the peak of competitive forgetting—as the ideal moment for SFT intervention. Our Annealed-RLVR algorithm is born from this insight. By applying a timed, corrective SFT shock, Annealed-RLVR mitigates the policy collapse and, as our experiments confirm, unlocks a superior final reasoning capability. Ultimately, this work provides a new lens for understanding RLVR: not as black-box optimization, but as a predictable process of structural self-organization, paving the way for more principled methods for engineering the advanced reasoning capabilities of future AI.

Looking forward, a central long-term goal is the empirical mapping of the complete, microscopic reasoning graph from large-scale foundation models. This remains a significant undertaking, requiring substantial computational resources and novel algorithms for semantic chunking and clustering. The payoff for this effort, however, would be transformative, producing a powerful new analytical object: a detailed map of an AI's internal world, composed of the reasoning graph and its emergent concept web. While the immediate application of this map would be to empirically test our sparse-web hypothesis, its long-term impact is far broader: charting this internal world is a critical step toward genuinely explainable LLMs and the robust safety of future artificial intelligence.

7 Related Work

Our work intersects with three domains: training paradigms for LLM reasoning, the modeling of reasoning as a complex network, and the study of RLVR's failure modes. While building on the standard RLVR paradigm (Guo et al., 2025; Team et al., 2025; Yang et al., 2025), our goal is to provide a theoretical-physics-motivated theory for its perplexing macroscopic dynamics. To this end, we engage with the view of reasoning as a complex network; however, our approach differs from prior work that empirically extracts static reasoning graphs post-hoc (Xiang et al., 2025; Cabannes et al., 2024; Minegishi et al., 2025). Inspired by the core logic of the RG, we bypass the intractable graph-construction challenge and instead hypothesize a simple organizational principle for the emergent, coarse-grained concept web with $\langle k \rangle \approx 2$, enabling us to study the universal behaviros of RLVR. This sparse-web perspective provides a unified origin for seemingly distinct failure modes like catastrophic forgetting (Li & Hoiem, 2017; Ding & Wang, 2025) and policy collapse (Yue et al., 2025; Cui et al., 2025), framing the former as the severing of the network's fragile bridges, and the latter as a consequence of a phase-transition-like learning dynamics at its frontier(Power et al., 2022; Lin et al., 2025; Cai et al., 2025). An important line of research has made valuable progress on these failures using algorithmic solutions (Chen et al., 2025). Our work contributes a complementary, theory-driven perspective: we leverage the sparse-web model to design Annealed-RLVR, an intervention that targets the problem's underlying structural root. See Appendix B for extended related work.

8 ACKNOWLEDGMENTS

The authors thank Haijun Zhou, Lei Wang, Hong Zhao and Ganqu Cui for inspiring discussions. K. C. and X. C. are supported by the National Key Research and Development Program of China under Grant No. 2024YFA1408604 and the National Natural Science Foundation of China under Grants No. 12047503 and No. 12447103. P. Z. is supported by Project 12325501 of the National Natural Science Foundation of China. Y. D. and S. H. are supported by the National Natural Science Foundation of China under Grants No. 12275263, the Innovation Program for Quantum Science and Technology under Grant No. 2021ZD0301900, and the Natural Science Foundation of Fujian Province of China under Grant No. 2023J02032. Z. Y. is supported by the National Natural Science Foundation of China under Grants No. 12304288 and No. 12247101.

9 Reproducibility Statement

To ensure full reproducibility, we provide a complete experimental blueprint in the Appendix: Sec. I details the LLM training pipeline—models, hyperparameters, and SFT dataset construction, while Sec. J describes our evaluation protocol. Our code repository of CoNet can be available at: https://anonymous.4open.science/r/CoNet-83A4. The repository includes a README.md file that details the functionality of each key Python script. The training process is described in Appendix D and Appendix H.

References

P. W. Anderson. More Is Different. *Science*, 177(4047):393–396, August 1972. doi: 10.1126/science.177.4047.393.

Albert-László Barabási and Réka Albert. Emergence of scaling in random networks. *science*, 286(5439): 509–512, 1999.

ByteDance Seed Team and verl community. verl: Volcano engine reinforcement learning for llms. `https://github.com/volcengine/verl`.

Vivien Cabannes, Charles Arnal, Wassim Bouaziz, Alice Yang, Francois Charton, and Julia Kempe. Iteration head: A mechanistic study of chain-of-thought, 2024. URL https://arxiv.org/abs/2406.02128.

Xiansheng Cai, Sihan Hu, Tao Wang, Yuan Huang, Pan Zhang, Youjin Deng, and Kun Chen. Learning-at-criticality in large language models for quantum field theory and beyond, 2025. URL https://arxiv.org/abs/2506.03703.

Zhipeng Chen, Xiaobo Qin, Youbin Wu, Yue Ling, Qinghao Ye, Wayne Xin Zhao, and Guang Shi. Pass@k training for adaptively balancing exploration and exploitation of large reasoning models, 2025. URL https://arxiv.org/abs/2508.10751.

Daixuan Cheng, Shaohan Huang, Xuekai Zhu, Bo Dai, Wayne Xin Zhao, Zhenliang Zhang, and Furu Wei. Reasoning with exploration: An entropy perspective on reinforcement learning for llms, 2025. URL https://arxiv.org/abs/2506.14758.

Ganqu Cui, Yuchen Zhang, Jiacheng Chen, Lifan Yuan, Zhi Wang, Yuxin Zuo, Haozhan Li, Yuchen Fan, Huayu Chen, Weize Chen, Zhiyuan Liu, Hao Peng, Lei Bai, Wanli Ouyang, Yu Cheng, Bowen Zhou, and Ning Ding. The entropy mechanism of reinforcement learning for reasoning language models, 2025. URL https://arxiv.org/abs/2505.22617.

Fei Ding and Baiqiao Wang. Improved supervised fine-tuning for large language models to mitigate catastrophic forgetting, 2025. URL https://arxiv.org/abs/2506.09428.

Subhabrata Dutta, Joykirat Singh, Soumen Chakrabarti, and Tanmoy Chakraborty. How to think step-by-step: A mechanistic understanding of chain-of-thought reasoning, 2024. URL https://arxiv.org/abs/2402.18312.

Ernesto Estrada and Naomichi Hatano. Subgraph centrality in complex networks. *Physical Review E*, 77(3): 036111, 2008.

Mehdi Fatemi, Banafsheh Rafiee, Mingjie Tang, and Kartik Talamadupula. Concise reasoning via reinforcement learning, 2025. URL https://arxiv.org/abs/2504.05185.

Heshan Fernando, Han Shen, Parikshit Ram, Yi Zhou, Horst Samulowitz, Nathalie Baracaldo, and Tianyi Chen. Mitigating forgetting in llm supervised fine-tuning and preference learning, 2025. URL https://arxiv.org/abs/2410.15483.

Javier Ferrando, Mehran Rezagholizadeh, and VS Dinesh Chandra Prabhu. A complex network approach to topic models, 2023.

Michael E. Fisher and Michael N. Barber. Scaling Theory for Finite-Size Effects in the Critical Region. *Physical Review Letters*, 28(23):1516–1519, June 1972. doi: 10.1103/PhysRevLett.28.1516.

Daya Guo, Dejian Yang, Haowei Zhang, Junxiao Song, Peiyi Wang, Qihao Zhu, Runxin Xu, Ruoyu Zhang, Shirong Ma, Xiao Bi, Xiaokang Zhang, Xingkai Yu, Yu Wu, Z. F. Wu, Zhibin Gou, Zhihong Shao, Zhuoshu Li, Ziyi Gao, Aixin Liu, Bing Xue, Bingxuan Wang, Bochao Wu, Bei Feng, Chengda Lu, Chenggang Zhao, Chengqi Deng, Chong Ruan, Damai Dai, Deli Chen, Dongjie Ji, Erhang Li, Fangyun Lin, Fucong Dai, Fuli Luo, Guangbo Hao, Guanting Chen, Guowei Li, H. Zhang, Hanwei Xu, Honghui Ding, Huazuo Gao, Hui Qu, Hui Li, Jianzhong Guo, Jiashi Li, Jingchang Chen, Jingyang Yuan, Jinhao Tu, Junjie Qiu, Junlong Li, J. L. Cai, Jiaqi Ni, Jian Liang, Jin Chen, Kai Dong, Kai Hu, Kaichao You, Kaige Gao, Kang Guan, Kexin Huang, Kuai Yu, Lean Wang, Lecong Zhang, Liang Zhao, Litong Wang, Liyue Zhang, Lei Xu, Leyi Xia, Mingchuan Zhang, Minghua Zhang, Minghui Tang, Mingxu Zhou, Meng Li, Miaojun Wang, Mingming Li, Ning Tian, Panpan Huang, Peng Zhang, Qiancheng Wang, Qinyu Chen, Qiushi Du,

Ruiqi Ge, Ruisong Zhang, Ruizhe Pan, Runji Wang, R. J. Chen, R. L. Jin, Ruyi Chen, Shanghao Lu, Shangyan Zhou, Shanhuang Chen, Shengfeng Ye, Shiyu Wang, Shuiping Yu, Shunfeng Zhou, Shuting Pan, S. S. Li, Shuang Zhou, Shaoqing Wu, Tao Yun, Tian Pei, Tianyu Sun, T. Wang, Wangding Zeng, Wen Liu, Wenfeng Liang, Wenjun Gao, Wenqin Yu, Wentao Zhang, W. L. Xiao, Wei An, Xiaodong Liu, Xiaohan Wang, Xiaokang Chen, Xiaotao Nie, Xin Cheng, Xin Liu, Xin Xie, Xingchao Liu, Xinyu Yang, Xinyuan Li, Xuecheng Su, Xuheng Lin, X. Q. Li, Xiangyue Jin, Xiaojin Shen, Xiaosha Chen, Xiaowen Sun, Xiaoxiang Wang, Xinnan Song, Xinyi Zhou, Xianzu Wang, Xinxia Shan, Y. K. Li, Y. Q. Wang, Y. X. Wei, Yang Zhang, Yanhong Xu, Yao Li, Yao Zhao, Yaofeng Sun, Yaohui Wang, Yi Yu, Yichao Zhang, Yifan Shi, Yiliang Xiong, Ying He, Yishi Piao, Yisong Wang, Yixuan Tan, Yiyang Ma, Yiyuan Liu, Yongqiang Guo, Yuan Ou, Yuduan Wang, Yue Gong, Yuheng Zou, Yujia He, Yunfan Xiong, Yuxiang Luo, Yuxiang You, Yuxuan Liu, Yuyang Zhou, Y. X. Zhu, Yanping Huang, Yaohui Li, Yi Zheng, Yuchen Zhu, Yunxian Ma, Ying Tang, Yukun Zha, Yuting Yan, Z. Z. Ren, Zehui Ren, Zhangli Sha, Zhe Fu, Zhean Xu, Zhenda Xie, Zhengyan Zhang, Zhewen Hao, Zhicheng Ma, Zhigang Yan, Zhiyu Wu, Zihui Gu, Zijia Zhu, Zijun Liu, Zilin Li, Ziwei Xie, Ziyang Song, Zizheng Pan, Zhen Huang, Zhipeng Xu, Zhongyu Zhang, and Zhen Zhang. DeepSeek-R1 incentivizes reasoning in LLMs through reinforcement learning. *Nature*, 645(8081):633–638, September 2025. ISSN 1476-4687. doi: 10.1038/s41586-025-09422-z.

Jujie He, Jiacai Liu, Chris Yuhao Liu, Rui Yan, Chaojie Wang, Peng Cheng, Xiaoyu Zhang, Fuxiang Zhang, Jiacheng Xu, Wei Shen, Siyuan Li, Liang Zeng, Tianwen Wei, Cheng Cheng, Bo An, Yang Liu, and Yahui Zhou. Skywork open reasoner series. `https://capricious-hydrogen-41c.notion.site/Skywork-Open-Reaonser-Series-1d0bc9ae823a80459b46c149e4f51680`, 2025. Notion Blog.

Dan Hendrycks, Collin Burns, Saurav Kadavath, Akul Arora, Steven Basart, Eric Tang, Dawn Song, and Jacob Steinhardt. Measuring mathematical problem solving with the math dataset. *NeurIPS*, 2021.

Hangzhan Jin, Sitao Luan, Sicheng Lyu, Guillaume Rabusseau, Reihaneh Rabbany, Doina Precup, and Mohammad Hamdaqa. Rl fine-tuning heals ood forgetting in sft, 2025. URL `https://arxiv.org/abs/2509.12235`.

Daniel Kahneman. *Thinking, fast and slow*. Farrar, Straus and Giroux, 2011.

Scott Kirkpatrick, C Daniel Gelatt Jr, and Mario P Vecchi. Optimization by simulated annealing. *science*, 220(4598):671–680, 1983.

Hanyu Lai, Xiao Liu, Yanxiao Zhao, Han Xu, Hanchen Zhang, Bohao Jing, Yanyu Ren, Shuntian Yao, Yuxiao Dong, and Jie Tang. Computerrl: Scaling end-to-end online reinforcement learning for computer use agents, 2025. URL `https://arxiv.org/abs/2508.14040`.

Aitor Lewkowycz, Anders Andreassen, David Dohan, Ethan Dyer, Henryk Michalewski, Vinay Ramasesh, Ambrose Slone, Cem Anil, Imanol Schlag, Theo Gutman-Solo, Yuhuai Wu, Behnam Neyshabur, Guy Gur-Ari, and Vedant Misra. Solving quantitative reasoning problems with language models, 2022.

Hongyu Li, Liang Ding, Meng Fang, and Dacheng Tao. Revisiting catastrophic forgetting in large language model tuning. In Yaser Al-Onaizan, Mohit Bansal, and Yun-Nung Chen (eds.), *Findings of the Association for Computational Linguistics: EMNLP 2024*, pp. 4297–4308, Miami, Florida, USA, November 2024. Association for Computational Linguistics. doi: 10.18653/v1/2024.findings-emnlp.249. URL `https://aclanthology.org/2024.findings-emnlp.249/`.

Huan Li, Ziqiao Liu, Yiding Li, and Qing-Fu Zhang. The emergence of essential structures in supervised learning. *Nature Communications*, 14(1):6483, 2023.

Zhizhong Li and Derek Hoiem. Learning without forgetting, 2017. URL `https://arxiv.org/abs/1606.09282`.

Yuchen Lin, Yong Zhang, Sihan Feng, and Hong Zhao. Network dynamics-based framework for understanding deep neural networks, 2025. URL https://arxiv.org/abs/2501.02436.

Zichen Liu, Changyu Chen, Wenjun Li, Penghui Qi, Tianyu Pang, Chao Du, Wee Sun Lee, and Min Lin. Understanding R1-Zero-Like Training: A Critical Perspective, March 2025.

Michael Luo, Sijun Tan, Justin Wong, Xiaoxiang Shi, William Y. Tang, Manan Roongta, Colin Cai, Jeffrey Luo, Li Erran Li, Raluca Ada Popa, and Ion Stoica. Deepscaler: Surpassing o1-preview with a 1.5b model by scaling rl. https://pretty-radio-b75.notion.site/DeepScaleR-Surpassing-O1-Preview-with-a-1-5B-Model-by-Scaling-RL-19681902c1468005bed8 2025. Notion Blog.

Aman Madaan, Niket Tandon, Prakhar Gupta, Kevin Hallinan, Luyu Gao, Sarah Wiegreffe, Uri Alon, Peter Andersen, Ishan Misra, Shubham Singh, et al. Self-refine: Iterative refinement with self-feedback. In *Advances in Neural Information Processing Systems*, volume 36, 2023.

Gouki Minegishi, Hiroki Furuta, Takeshi Kojima, Yusuke Iwasawa, and Yutaka Matsuo. Topology of reasoning: Understanding large reasoning models through reasoning graph properties, 2025.

Alethea Power, Yuri Burda, Harri Edwards, Igor Babuschkin, and Vedant Misra. Grokking: Generalization beyond overfitting on small algorithmic datasets, 2022. URL https://arxiv.org/abs/2201.02177.

Zhihong Shao, Peiyi Wang, Qihao Zhu, Runxin Xu, Junxiao Song, Xiao Bi, Haowei Zhang, Mingchuan Zhang, Y. K. Li, Y. Wu, and Daya Guo. DeepSeekMath: Pushing the Limits of Mathematical Reasoning in Open Language Models, April 2024. URL http://arxiv.org/abs/2402.03300. arXiv:2402.03300 [cs].

Idan Shenfeld, Jyothish Pari, and Pulkit Agrawal. Rl's razor: Why online reinforcement learning forgets less, 2025. URL https://arxiv.org/abs/2509.04259.

Guangming Sheng, Chi Zhang, Zilingfeng Ye, Xibin Wu, Wang Zhang, Ru Zhang, Yanghua Peng, Haibin Lin, and Chuan Wu. Hybridflow: A flexible and efficient rlhf framework. *arXiv preprint arXiv: 2409.19256*, 2024.

Noah Shinn, Beck Labash, and Roger Grosse. Reflexion: An autonomous agent with dynamic memory and self-reflection, 2023.

Harry Eugene Stanley and Guenter Ahlers. Introduction to phase transitions and critical phenomena. *American Journal of Physics*, 40:927–928, 1972. URL https://api.semanticscholar.org/CorpusID:10416417.

Kimi Team, Angang Du, Bofei Gao, Bowei Xing, Changjiu Jiang, et al. Kimi k1.5: Scaling Reinforcement Learning with LLMs, March 2025.

Jesse Vig. A multiscale visualization of attention in the transformer model, 2019.

Xinyi Wang, Alfonso Amayuelas, Kexun Zhang, Liangming Pan, Wenhu Chen, and William Yang Wang. Understanding reasoning ability of language models from the perspective of reasoning paths aggregation, 2024. URL https://arxiv.org/abs/2402.03268.

Xuezhi Wang, Jason Wei, Dale Schuurmans, Quoc Le, Ed Chi, Sharan Narang, Aakanksha Chowdhery, and Denny Zhou. Self-consistency improves chain of thought reasoning in language models, 2022.

Duncan J Watts and Steven H Strogatz. Collective dynamics of 'small-world'networks. *nature*, 393(6684): 440–442, 1998.

Jason Wei, Xuezhi Wang, Dale Schuurmans, Maarten Bosma, Ed Chi, Quoc Le, and Denny Zhou. Chain-of-thought prompting elicits reasoning in large language models. In *Advances in Neural Information Processing Systems*, volume 35, pp. 24824–24837, 2022.

K. G. Wilson and John B. Kogut. The Renormalization group and the epsilon expansion. *Phys. Rept.*, 12: 75–199, 1974. doi: 10.1016/0370-1573(74)90023-4.

Kenneth G. Wilson. The renormalization group and critical phenomena. *Reviews of Modern Physics*, 55(3): 583–600, July 1983. doi: 10.1103/RevModPhys.55.583.

Violet Xiang, Charlie Snell, Kanishk Gandhi, Alon Albalak, Anikait Singh, Chase Blagden, Duy Phung, Rafael Rafailov, Nathan Lile, Dakota Mahan, Louis Castricato, Jan-Philipp Franken, Nick Haber, and Chelsea Finn. Towards system 2 reasoning in llms: Learning how to think with meta chain-of-thought, 2025. URL https://arxiv.org/abs/2501.04682.

An Yang, Anfeng Li, Baosong Yang, Beichen Zhang, Binyuan Hui, et al. Qwen3 technical report. *arXiv preprint arXiv:2505.09388*, 2025.

Shunyu Yao, Dian Yu, Jeffrey Zhao, Izhak Sha, Silvio Savarese, and an an. Tree of thoughts: Deliberate problem solving with large language models, 2023.

Qiying Yu, Zheng Zhang, Ruofei Zhu, Yufeng Yuan, Xiaochen Zuo, et al. DAPO: An Open-Source LLM Reinforcement Learning System at Scale, March 2025. URL http://arxiv.org/abs/2503.14476. arXiv:2503.14476 [cs] version: 1.

Yang Yue, Zhiqi Chen, Rui Lu, Andrew Zhao, Zhaokai Wang, Yang Yue, Shiji Song, and Gao Huang. Does reinforcement learning really incentivize reasoning capacity in llms beyond the base model?, 2025. URL https://arxiv.org/abs/2504.13837.

A The Use of Large Language Models (LLMs)

This work utilized Large Language Models (LLMs) to assist in the preparation of the manuscript, primarily for improving language clarity and readability. For the accompanying CoNet repository, we also employed LLMs to generate Python codes, such as the training algorithm, measuring network properties and visualizing the concept web and its largest connected component. All LLM-generated outputs, including text and code, were meticulously reviewed, edited, and verified by the authors to ensure their accuracy and suitability for this work.

B Extended Related Work

System-2 Reasoning in LLMs. The dual-process theory, distinguishing between fast, intuitive System-1 thinking and slow, deliberate System-2 reasoning (Kahneman, 2011), has become a valuable framework for analyzing LLM behavior. While standard LLMs often exhibit System-1-like responses, significant research has focused on eliciting more robust, System-2 deliberation. Prompting strategies such as Chain-of-Thought (CoT) (Wei et al., 2022) and its variants like Self-Consistency (Wang et al., 2022) and Tree of Thoughts (ToT) (Yao et al., 2023) encourage models to generate explicit reasoning steps. Other works aim to build this deliberative capacity into the model's architecture or training process through self-correction and reflection (Shinn et al., 2023; Madaan et al., 2023). Our work complements these efforts by shifting the

focus from **eliciting** reasoning to understanding the **emergent mechanism** of how this capability develops internally during training.

Complex Network Analysis of Neural Models. Applying network science to understand neural networks is a long-standing idea, previously used to study the topology and robustness of smaller models (Estrada & Hatano, 2008). With the advent of Transformers, researchers have begun analyzing attention patterns as graphs (Vig, 2019; Ferrando et al., 2023) to better understand information flow. More recently, studies have explored how network structures emerge during supervised learning, identifying the formation of essential subnetworks (Li et al., 2023). A recent study by (Minegishi et al., 2025) shares our goal of analyzing the network structures that underpin System-2 reasoning, though they do so by empirically extracting a graph from hidden-state representations. In contrast, our CoNet framework utilizes a fixed, abstract concept space, which allows us to specifically isolate and analyze the dynamic mechanism of how this reasoning structure emerges during training.

C The Reasoning Graph: From Empirical Extraction to a Unified Concept Web

The idea of a reasoning graph has emerged in the literature as a powerful framework for understanding the chain-of-thought process in LLMs for a given task. This graph is not explicitly encoded in the Transformer's static parameters but is an emergent property of its inference dynamics. The standard model for its construction is based on a key observation: an LLM's generative process is guided by a few decision points of high Shannon entropy, or "forking tokens" (Fig. 7). This allows for a deconstruction of a chain-of-thought: stable, low-entropy text chunks form the graph's nodes (concepts), while the probabilistic choices at these high-entropy forks form the weighted, directed edges.

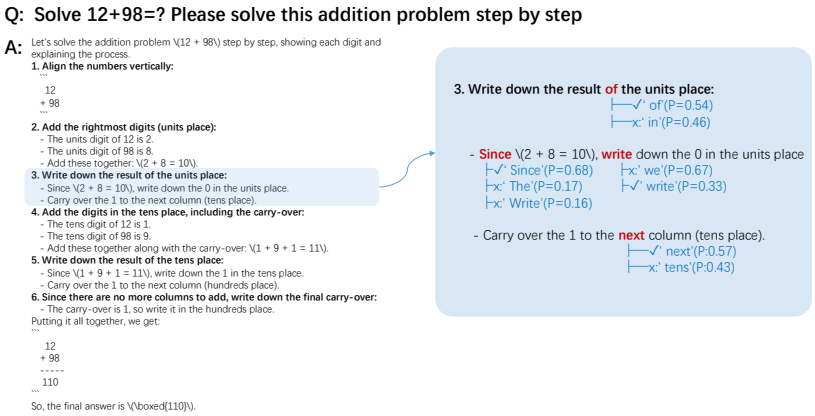

Figure 7: Illustration of the LLM reasoning process. A chain-of-thought is composed of stable, low-entropy text chunks (concepts), connected by high-entropy 'forking tokens' that represent decision points. The LLM reasoning process can be deconstructed into stable "concepts" (e.g., step 3) linked by high-entropy decision points. The probabilities at these junctures (e.g., "next" vs. "tens") represent transition weights on an underlying reasoning graph, a view supported by convergent findings on the role of high-entropy tokens.

Recent work, notably by (Minegishi et al., 2025), has developed detailed methods to empirically construct these task-specific reasoning graphs. Their process involves generating a large corpus of reasoning chains, segmenting them into individual steps, and then computing a vector representation for each step by averaging

the hidden states of its tokens at a specific Transformer layer. Finally, a clustering algorithm (e.g., K-means) is used on the full set of step vectors, with the resulting cluster centroids being defined as the graph's nodes. By analyzing graphs constructed this way, they found that more advanced models exhibit distinct topological properties, such as larger diameters, which correlate with improved performance.

While analyzing these static, task-specific graphs is insightful, it leads to a deeper question: what is the underlying, universal knowledge structure that allows an LLM to generate so many different reasoning graphs across a multitude of tasks? It follows that these empirically observed reasoning graphs are best understood as small projections of a much vaster, latent concept web. This web represents the entirety of the model's abstract knowledge, and the ultimate goal is to understand its structure.

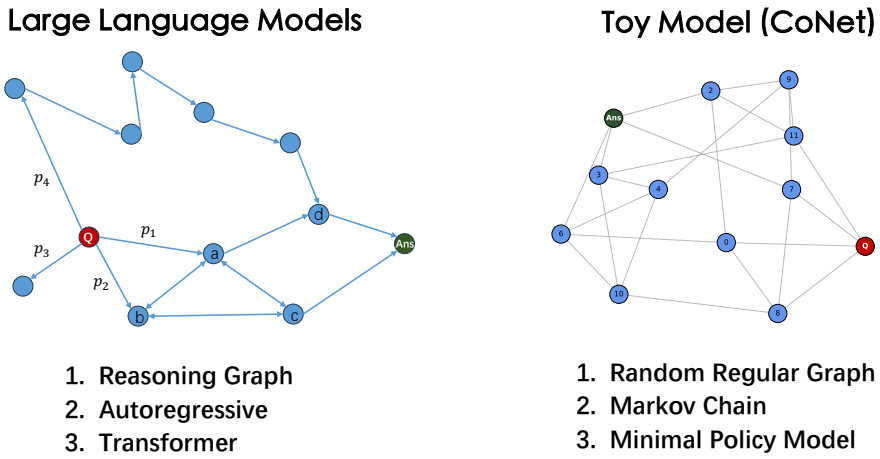

Figure 8: **From Intractable LLM Dynamics to a Minimal CoNet Model.** The reasoning process in an LLM (left) can be viewed as a traversal on a high-dimensional latent graph, where path probabilities are determined by the complex, autoregressive Transformer. Directly analyzing this graph's evolution is intractable. CoNet (right) provides a minimal abstraction by replacing the intractable latent graph with a fixed K-regular random graph and simplifying the generation policy to a learnable Markov chain. This creates a tractable "computational microscope" to precisely analyze how the transition policy evolves under reinforcement, isolating the core dynamics of reasoning path formation.

However, attempting to reverse-engineer this universal concept web from its sparse, task-specific projections presents formidable obstacles. The difficulties are multi-fold. First is a problem of scale: the true concept web is of astronomical size, and any extracted graph is an infinitesimal sample. More fundamentally is the ambiguity of the concept mapping: the mapping from a low-level token sequence to a high-level semantic concept is inherently many-to-one. Finally, this already-ambiguous mapping is itself dynamic, as it can shift during RLVR training. These challenges collectively lead to the observable node stability problem in practice, making it nearly impossible with current methods to track the web's true topological evolution.

It is precisely this observational challenge that our paper bypasses with a two-pronged, indirect approach. First, we form a theoretical hypothesis about the consequences of a specific topological structure (i.e., sparsity). Second, we use a minimal model (CoNet) that captures the essential physics of the system to study these consequences in a controlled environment. Thus, while the direct construction of the concept web remains an open problem, our work proceeds from a central hypothesis about its fundamental structure. This Hypothesis—that the web is profoundly sparse with an average degree near two—serves as the theoretical foundation for our paper. From it, we first demonstrate how this assumption of sparsity explains

the known macroscopic dynamics of RLVR. We then use it to deduce previously overlooked microscopic mechanisms, namely frustration-induced forgetting and phase-transition-like learning. Finally, armed with these new insights, we explore how this deeper understanding can be leveraged to design a novel, improved RLVR algorithm.

D CoNet: A Minimal Model for RLVR dynamics

To bypass the intractable node stability problem, we leverage the Concept Network Model (CoNet). CoNet was originally introduced in (Cai et al., 2025) to study the dynamics of single-task RLVR, but its core design makes it perfectly suited for our investigation. By positing a fixed space of concept nodes (a static graph structure) and isolating all learning dynamics to the evolving policy that navigates it, CoNet allows us to sidestep the challenges of direct graph extraction and precisely measure how the reinforcement signal sculpts reasoning paths. The model represents the LLM's concept space as an abstract K-regular random graph, with the reasoning process simplified to a policy-guided Markovian random walk, as shown in Fig.8. The transition policy, $\pi_\theta(j|i) \propto \theta_{ij}$, is governed by a set of learnable parameters θ_{ij} that represent the strength of the connection from node i to node j. This policy is updated via RLVR on successful paths from a question (Q) to an answer (A).

This design offers a clear cognitive analogy. A single-step hop on the graph represents "System 1" thinking—fast, intuitive associations. A multi-step traversal, guided by the learned policy, represents "System 2" reasoning—a deliberate, compositional chain of thought. It is crucial to note that CoNet is not a model of the Transformer's parameters themselves; rather, it models the emergent semantic network induced by inference—the structure that governs how questions are connected to answers through chains of concepts.

CoNet was originally introduced to model the phenomenon of Learning at Criticality (LaC), which was identified in single-task RLVR training (Cai et al., 2025). The central finding of LaC is that for a model trained on extremely sparse data (e.g., a single exemplar), generalization performance on unseen problems peaks precisely at a sharp, sigmoidal learning transition, before declining due to overfitting. The original work used CoNet to establish that this dynamic is a learning phase transition, providing a physical model for this peak in generalization.

The central methodological advance of this paper is to deploy this existing model in a richer, multi-task setting with numerous concurrent Q-A pairs. This extension is crucial: it transforms CoNet from a model of isolated skill acquisition into an ideal theoretical laboratory for studying skill integration. In this regime, the model is compelled by competing reinforcement signals to discover a shared, reusable structure. As Fig. 1 shows, this multi-task CoNet stunningly reproduces the key macroscopic signatures of the 1.5B LLM. This correspondence validates our use of CoNet as a minimal model for exploring the network-level mechanisms of frustration and web formation.

CoNet was originally introduced to model the phenomenon of Learning at Criticality (LaC), which was identified in single-task RLVR training (Cai et al., 2025). The central finding of LaC is that for a model trained on extremely sparse data, generalization performance peaks precisely at a sharp learning transition. The key methodological advance of this paper is to deploy this model in a richer, multi-task setting. This extension is crucial: it transforms CoNet from a model of isolated skill acquisition into an ideal theoretical laboratory for studying the emergent phenomena of skill integration, frustration, and concept web formation. As Fig. 1 shows, this multi-task CoNet stunningly reproduces the key macroscopic signatures of the 1.5B LLM, validating its use for exploring the network-level mechanisms that drive the emergence of reasoning.

E CoNet Implementation Details

We configured CoNet with a specific set of structural and learning parameters. The underlying concept space was instantiated as a directed random regular graph with $N = 800$ nodes, where each node has a uniform out-degree of $k = 40$. In this graph, we established a multi-task learning environment consisting of 128 randomly generated question-answer (Q-A) node pairs. The initial transition parameters θ_{ij} for all edges were assigned randomly. The use of a multi-task setting with 128 concurrent Q-A pairs is the fundamental mechanism that induces structural competition. While a single task would only require finding one efficient path, the presence of numerous tasks provides competing reinforcement signals. When multiple Q-A paths need to traverse a common node, they may "disagree" on the optimal subsequent step, leading to conflicting policy updates. This microscopic conflict is the origin of the macroscopic "frustration" discussed in the main text, compelling the system to find a shared, globally coherent structure that can arbitrate these conflicts, rather than settling for 128 disconnected "skill islands".

The policy was optimized using a variant of the Group Relative Policy Optimization (GRPO) algorithm ((Shao et al., 2024; Liu et al., 2025; Yu et al., 2025)). For a given Q-A pair, $n_{\text{rollout}} = 128$ reasoning paths (indexed by m) were sampled, with each path's exploration capped at a maximum length of 20 steps. Each path received a reward based on its success, and its advantage A_m (relative to the average reward over all 128 rollouts) was used to guide the update of the policy parameters θ_{ij}. The update rule is given by:

$$\Delta\theta_{ij} \propto \sum_m A_m \nabla_{\theta_{ij}} \log \pi_\theta(j|i)$$

This advantage-based update functions as a competitive reinforcement mechanism. Only paths performing better than the current average are strengthened, while underperforming paths are implicitly suppressed. This "winner-take-more" dynamic acts as an algorithmic sculpting tool, systematically pruning the vast majority of the initial $k = 40$ edges from each node to carve out the sparse, efficient backbone of the concept web. The learning rate was set to 0.04 to control the speed and stability of this training process.

Crucially, the two-stage learning dynamic is not an artifact of fine-tuned parameters but a robust emergent property of the model. Repeated experiments show that this behavior—a fast-learning phase followed by a slow integration plateau, and the corresponding V-shaped response length—consistently emerges under a broad condition: when the number of Q-A pairs, N_{QA}, is in the regime of $1 \ll N_{QA} \ll N$. This dynamic is qualitatively different from the single Q-A pair ($N_{QA} = 1$) case, which produces a simple sigmoidal learning transition (the LaC phenomenon). The condition is essential: if N_{QA} is too small, there is no systemic competition to drive the formation of a unified web; if it is too large, the conflicting reinforcement signals prevent any coherent structure from forming. The robust emergence of these LLM-like signatures in this intermediate regime confirms that our CoNet setup successfully isolates the core principles of structural self-organization under multi-task reinforcement.

F Structural Evolution of the Concept Web in CoNet

This section provides direct, quantitative evidence from the CoNet model for the two-stage learning dynamic—a fast acquisition phase followed by a slow integration phase—that underlies our theory. Fig. 9 serves as the central exhibit for this analysis, tracking two key structural properties over the course of training: the total number of disconnected solution clusters (the "skill islands") and the size of the single largest cluster, namely the concept web.

The first stage of training ($\sim$ 0-50 steps), corresponding to the fast-learning phase, is characterized by the rapid proliferation of "skill islands". The quantitative evidence for this is the steep, initial rise of the "Cluster Number" (orange curve) in Fig. 9. Each new cluster represents the discovery of a distinct, high-confidence

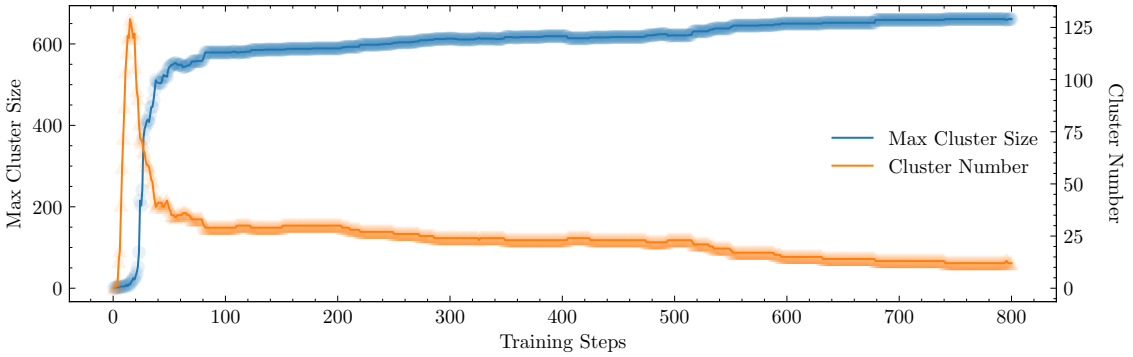

Figure 9: **The Formation of the Concept Web in CoNet.** This figure illustrates the evolution of network clusters during training, showing a structural transition from isolated skills to a unified conceptual web. In the initial phase, the Cluster Number (orange curve) spikes, indicating the rapid discovery of numerous disconnected "skill islands". The peak marks a critical transition point. Following this peak, the Cluster Number steadily declines as these islands begin to coalesce. This merging process is confirmed by the corresponding monotonic growth in the Max Cluster Size (blue curve), which represents the formation of a single giant component. By the end of training, the network is dominated by this large, interconnected structure.

reasoning path for a specific problem. During this phase, the system operates in a greedy, parallel fashion, finding many efficient, local solutions without regard for their interconnection.

The transition to the slow-learning phase occurs at the critical juncture marked by the peak of the orange curve around step 20. At this point, the system has exhausted the "low-hanging fruit" of simple, isolated solutions and has reached a state of maximal fragmentation. This peak signals the onset of the "maximally frustrated state" discussed in the main text. The subsequent, gradual decline of the "Cluster Number" curve is the direct signature of this frustrated state, representing the arduous and competitive process of integrating existing islands rather than discovering new ones. The "Max Cluster Size" (blue curve), which begins its steep, sustained ascent at precisely this moment, confirms this shift from local discovery to a global integration objective.

The slow-learning phase is thus defined by the coalescence of these islands into a unified concept web. The plot reveals the two complementary trends that define this stage: a steady decline in the total number of clusters (orange curve) and a simultaneous, relentless growth in the size of the largest cluster (blue curve). The causal link is direct: the largest component grows precisely by absorbing smaller, independent clusters, which necessarily reduces the total cluster count. This structural evolution culminates in a state where a single, giant component—the functional concept web—dominates the network. This process provides a direct, mechanical explanation for the V-shaped response length signature: Stage 1 shortens paths by finding local solutions, while Stage 2 lengthens them by forcing the policy to traverse longer, connective paths between previously distant concepts.

G Learning by Phase Transition in the Slow-Learning Stage

In the main text, we argue that new knowledge acquisition during the slow-learning stage is not gradual but occurs via discrete, sharp events. This appendix provides detailed, per-problem evidence for this learning by phase transition mechanism, drawing a direct analogy to critical phenomena in statistical physics.

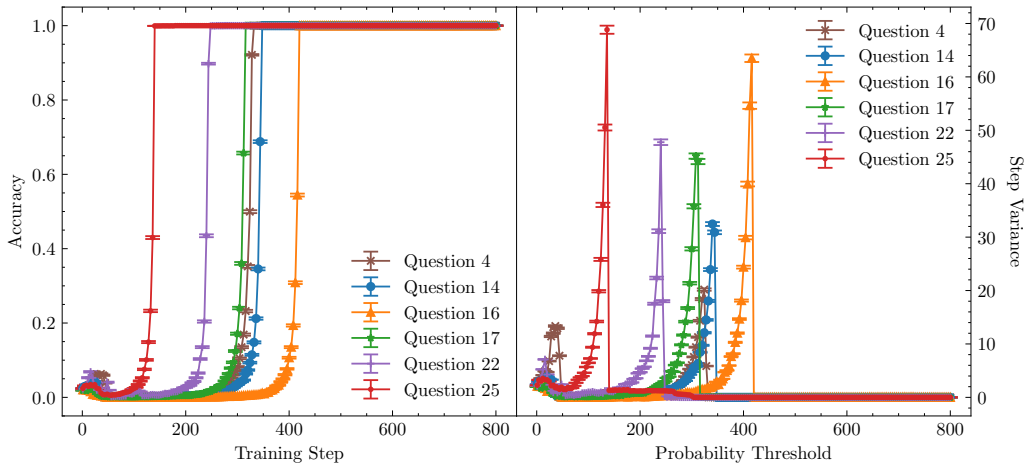

Figure 10: **Per-Problem Critical Dynamics During the Slow-Learning Stage.** These plots reveal the microscopic learning dynamics for a representative subset of problems that successfully learn during the slow-learning stage, providing evidence for localized phase transitions. **(Left)** Accuracy trajectories for these problems. All problems shown exhibit a sharp, sigmoidal-like increase in accuracy late in the training process, characteristic of a critical learning event. **(Right)** Corresponding variance of the solution path length. A sharp, pronounced peak in variance directly coincides with the rapid accuracy gain for each problem. This dual signature is the hallmark of a continuous phase transition, suggesting that the slow-learning stage in CoNet is composed of discrete, sharp learning events rather than a uniform, gradual process.

Fig. 10 isolates a representative subset of problems mastered late in the training process. The first signature of a phase transition is visible in the left panel: each problem exhibits a sharp, sigmoidal-like jump in accuracy. In the language of statistical physics, accuracy acts as an order parameter, signaling the system's transition from a disordered (unsolved) state to an ordered (solved) state. An abrupt change in the order parameter is a primary indicator of a phase transition.

The second, more telling signature is the pronounced, transient peak in the variance of the solution path length, shown in the right panel. This provides a deeper link to the physics of critical phenomena. In physical systems, the variance (or fluctuations) of an order parameter is related to the system's susceptibility—its response sensitivity to external perturbations. At the critical point of a continuous phase transition, this susceptibility is known to diverge, creating a characteristic sharp peak. A famous example of this is the lambda (λ) peak observed in the specific heat of liquid helium at the normal-to-superfluid transition. The variance peaks in our figure are the direct analogue of this phenomenon. This "dual signature"—an abrupt rise in the order parameter (accuracy) and a lambda-like peak in its fluctuations (variance)—is the classic hallmark of a critical learning transition. This same analysis was performed in the original work on LaC, where the variance peak in the single-task CoNet was identified as a key hallmark of a learning phase transition (Cai et al., 2025).

The intuitive reason for this variance peak is straightforward. When accuracy is very low, nearly all sampled paths fail, resulting in low variance. When accuracy is very high, the model has converged on a dominant, efficient reasoning path, again leading to low variance. It is only during the narrow transition window that a rich diversity of paths coexists—some still failing, while others explore newly viable routes to the solution. This temporary coexistence of competing strategies is what produces the characteristic peak in variance.

Taken together, these results provide strong microscopic validation for our claims. They show that the slow-learning stage in CoNet is not a process of uniform, gradual improvement. Instead, it is punctuated by a series of discrete, critical learning events, where individual skills are integrated into the concept web one by one via localized phase transitions at the frontier.

H THE SFT AND ANNEALED-RLVR ALGORITHM IN CONET

This appendix details the implementation and validation of the Annealed-RLVR algorithm in CoNet, our "computational microscope" for LLM reasoning dynamics. The algorithm is designed to intervene at the point of "maximum frustration" with SFT to resolve the competitive bottlenecks that arise during the formation of the sparse concept web.

H.1 SFT IMPLEMENTATION IN CONET

CoNet's minimalistic policy model significantly simplifies the standard SFT process. This process involves first using the original model's policy to sample a successful reasoning path for a given problem. Then, for this selected path, we adjust its transition probabilities. For any transition on the path with a probability below a certain threshold, we raise it to that threshold value. To ensure that the probability distribution of each node remains valid, the probabilities of other outgoing transitions are proportionally reduced. The value of this target transition probability is a tunable parameter that determines the intervention's effect. For our annealing strategy, we set this value to 0.1. To induce catastrophic forgetting, we use a more aggressive value of 0.5.

H.2 EXPEIMENTAL RESULTS

The algorithm consists of a strategically timed Supervised Fine-Tuning (SFT) phase, followed by a resumption of standard Reinforcement Learning from Verifiable Rewards (RLVR) training. The SFT intervention is applied at training step 50, the empirically determined point of maximum frustration where the system transitions from forming disconnected "skill islands" to integrating them. At this stage, we first identify all problems with an accuracy below 0.1, select a total of 50 low-accuracy problems, and sample a known successful reasoning path for each. This targeted adjustment serves as the "heating" step in our simulated annealing analogy; it gently increases the discoverability of latent correct paths to restore the system's exploratory capacity. Following this brief SFT, standard RLVR training is resumed, which functions as the "cooling" phase, allowing the now more exploratory policy to settle into a new, more globally optimal configuration.

The success of this SFT-RLVR cycle is confirmed by the results in Fig. 11. The line plot on the right shows the immediate effect of the intervention: best@1 accuracy (a proxy for exploitation) temporarily dips, while best@16 accuracy (a proxy for exploration) surges. This demonstrates a successful trade of greedy exploitation for enhanced exploration, and the long-term benefit is clear, as the final annealed policy significantly surpasses the baseline RLVR policy. The histogram on the left reveals the underlying mechanism for this improvement. The SFT-RLVR cycle successfully resolves the frustration bottleneck by dramatically reducing the population of completely unsolved problems (Accuracy = 0.0) and correspondingly increasing the number of fully mastered problems (Accuracy = 1.0) compared to the standard model.

In summary, the CoNet experiment provides strong evidence for our theory. By applying a targeted and conservative SFT intervention at the point of maximum frustration, the Annealed-RLVR algorithm effectively resolves the system's competitive bottlenecks, enabling it to discover a more robust and better reasoning policy.

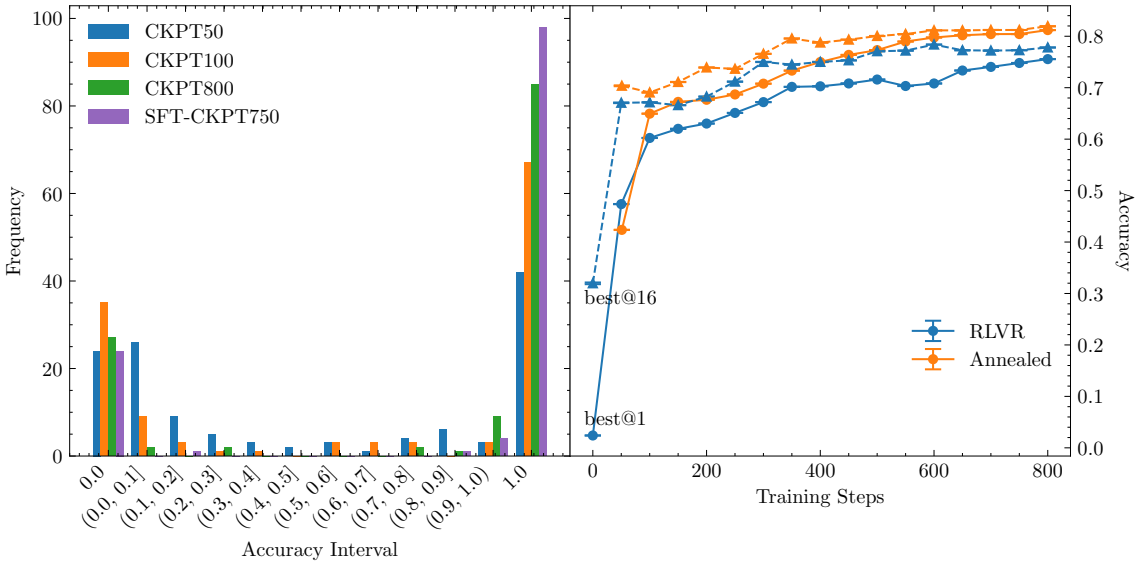

Figure 11: **Validation of Annealed-RLVR in CoNet. (Left)** The histogram of per-problem accuracy shows that the annealed model (SFT-CKPT750) significantly reduces the number of completely unsolved problems (Accuracy = 0.0) and increases the number of mastered problems (Accuracy = 1.0) compared to the standard model (CKPT800). **(Right)** The line plot of training dynamics shows that immediately after the SFT intervention at step 50, best@1 accuracy dips while best@16 accuracy sharply increases, indicating a successful trade of exploitation for exploration. The final annealed policy ("Annealed") ultimately achieves superior performance over the baseline ("RLVR").

I LLM Training Details

I.1 Base Model and GRPO Setup

We used the **DeepSeek-R1-Distill-Qwen-1.5B** model (Guo et al., 2025), trained on the DeepScaleR-Preview-Dataset (Luo et al., 2025) with their modified version of the veRL open-source engine (Sheng et al., 2024; ByteDance Seed Team and verl community). Our Generative Reward Policy Optimization (GRPO) hyperparameters followed the first-stage settings, which specified a response length of 8192, as outlined in the DeepScaleR paper (Luo et al., 2025).

I.2 SFT Dataset for Annealed-RLVR

The Supervised Fine-Tuning (**SFT**) dataset for the **annealed-RLVR** experiment (labeled "Annealed" in Fig. 6) was constructed to focus on difficult problems. First, we trained the base model using GRPO for 100 steps to create a checkpoint (CKPT100), which is in the vicinity of the maximally frustrated state. We then used this checkpoint to generate 8 rollouts for each of the approximately 40,000 problems in the training set. For the roughly 10,000 problems that yielded no correct responses, we generated an additional 52 rollouts, bringing the total to 60 per problem. From this data, we created the SFT dataset by selecting all correct responses for problems where the initial model accuracy was below 10%, which yielded **3,933 trajectories**. Finally, we fine-tuned the model on these trajectories for two epochs with a learning rate of 3×10^{-5}. The resulting model served as the new starting point for continuing GRPO training up to step 1,700.

I.3 SFT Dataset for Catastrophic Forgetting

The SFT dataset for the **catastrophic forgetting** experiment (labeled "SFT+RLVR" in Fig. 4(b)) was designed to specifically target problems forgotten by a more saturated model, using a data generation process that involved multiple checkpoints. The process began with problem filtering: we used a checkpoint from step 600 (CKPT600, deep within the slow-learning stage) to generate 8 rollouts for all training problems. We then identified the subset of problems with no correct responses and generated another 32 rollouts for them, again using CKPT600. Problems that still had no correct responses were selected as the final "forgotten" set. For the second stage of targeted data generation, each problem in this forgotten set was used to generate a total of 96 rollouts: 32 from the **base model**, 32 from CKPT100, and 32 from CKPT600. We then collected correct responses from problems that had at least 3 correct answers among these 96 rollouts, resulting in **798 trajectories**. This SFT dataset was used to fine-tune the model for two epochs with a learning rate of 5×10^{-5} before resuming GRPO training.

J LLM Evaluation Details

We evaluated checkpoints from our RLVR ("GRPO") and annealed-RLVR ("Annealed") training runs on two datasets: 512 randomly selected training problems and the Minerva math dataset (Hendrycks et al., 2021; Lewkowycz et al., 2022). The evaluation parameters were kept consistent with the training configuration (temperature: 0.6, top-p: 1.0, response length: 8192, etc.). From the 512 rollout results, we calculated the best@k accuracy and the standard error. Fig. 6 illustrates the full performance curves, while Table 1 highlights the results from representative checkpoints.

Table 1: Best@k Accuracy (%) with Standard Error at Key Training Checkpoints

Metric	Method	Checkpoints (Steps)						
		0	**100**	**200**	**600**	**1000**	**1400**	**1800**
Dataset: Randomly Selected 512 Training Problems								
best@1	GRPO	43.66(6)	50.17(6)	52.45(6)	56.49(6)	58.00(6)	58.90(6)	59.55(6)
	Annealed	—	50.00(6)	52.27(6)	55.80(6)	58.10(6)	59.46(6)	**60.31(6)**
best@4	GRPO	61.32(8)	68.46(8)	70.38(8)	72.99(7)	73.46(7)	73.71(7)	74.20(7)
	Annealed	—	69.49(8)	71.51(8)	73.75(7)	75.10(7)	75.91(7)	**76.77(7)**
best@16	GRPO	72.97(12)	78.60(11)	80.12(11)	81.60(10)	81.61(10)	81.62(10)	81.86(10)
	Annealed	—	80.62(11)	82.22(11)	83.15(10)	83.77(10)	84.48(10)	**85.28(10)**
best@128	GRPO	82.16(24)	86.98(23)	87.81(20)	87.47(19)	88.23(21)	87.77(19)	87.99(22)
	Annealed	—	88.00(19)	89.35(20)	89.37(19)	89.98(18)	90.23(18)	**91.22(18)**
Dataset: Minerva								
best@1	GRPO	23.85(7)	26.08(7)	26.83(7)	27.63(7)	28.53(7)	28.45(7)	28.77(7)
	Annealed	—	26.09(7)	26.62(7)	27.73(7)	28.28(7)	28.75(7)	**28.88(7)**
best@4	GRPO	37.84(12)	40.77(12)	41.33(12)	41.12(12)	41.46(11)	41.04(11)	41.32(11)
	Annealed	—	40.63(12)	40.90(12)	41.66(12)	42.04(11)	**42.53(11)**	42.39(11)
best@16	GRPO	51.39(21)	**54.29(21)**	54.20(21)	53.05(20)	52.38(19)	52.12(20)	51.95(19)
	Annealed	—	53.80(21)	53.71(21)	53.74(20)	53.86(21)	54.24(21)	53.50(20)
best@128	GRPO	66.6(5)	68.8(4)	**69.8(5)**	66.2(4)	65.8(5)	64.9(4)	64.4(4)
	Annealed	—	68.2(5)	68.3(4)	68.4(5)	68.0(4)	69.4(5)	67.8(5)